Ecology, 61(3), 1980, pp. 562–571

FLOW ANALYSIS OF MODELS OF THE HUBBARD BROOK ECOSYSTEM[1]

JOHN T. FINN
Department of Forestry and Wildlife Management, University of Massachusetts, Amherst, Massachusetts 01003 USA

Abstract. Several models of energy and nutrient flow on the Hubbard Brook Ecosystem, New Hampshire, USA, were analyzed for the pattern of flow through the models, cycling index *CI*, path length $\overline{PL}$, and straight-through path length $\overline{PL}_s$. *CI* represents the proportion of flow that cycles through components of the system. $\overline{PL}$ is the average number of components that a unit of flow passes through on its way from inflow to outflow. $\overline{PL}_s$ is that portion of $\overline{PL}$ attributable to flow passing straight through the system without cycling at all. The energy model had low values for $\overline{PL}$, $\overline{PL}_s$, and *CI*, compared to nutrient models. Flow measures for nutrients varied greatly. The order of the elements in terms of *CI* was K > Na > N > Ca > P > Mg > S. This could be explained by the mobility and biological role of each element, although Na is somewhat anomalous. $\overline{PL}$ was very large for K (24.3) but small for S (5.2). $\overline{PL}_s$ was near 4 for all elements but Na (2.6) and S (2.5). This was a reflection of different flow patterns for Na, which flows primarily between available nutrients and belowground biomass, and S, which flows primarily between available nutrients, and below- and aboveground biomass. Sulfur returns to available nutrients via stemflow and throughflow, bypassing the forest floor. The remaining elements cycle between above- and belowground biomass, forest floor, and available nutrients.

Three different models of Ca flow were compared. When all three models were analyzed using the same nutrient flux data, flow measures became very close, despite structural differences in the models. For these models, flow values were more important than the architecture of the models in determining cycling and flow characteristics.

Key words: cycling index; energy flow; flow analysis; Hubbard Brook; nutrient cycling; path length.

INTRODUCTION

Hubbard Brook is one of the best studied ecosystems in the world. A great deal is known about successional sequence, nutrient cycling, and energy flow on the several watersheds that comprise the Hubbard Brook Ecosystem. This paper applies flow analysis, a method of tracing flows of materials through a system, to some of the Hubbard Brook data to determine (1) the amount cycled per year of several elements and energy at Hubbard Brook compared to the total amount of each flowing per year in the system and (2) the pattern of nutrient and energy flow in the ecosystem. In addition, three different models of Ca flow are compared to judge the effect of small differences in model structure on cycling and flow pattern.

FLOW ANALYSIS METHODS

Flow analysis techniques were originally borrowed from economic input-output analysis and have been described in detail by several authors (Hannon 1973, Cale 1975, Finn 1976, 1977, 1978, Patten et al. 1976, Barber 1978*a,b,* Patten and Finn 1979). Here I will briefly describe the flow analysis measures used and forego formal derivation of those measures. The methods will be described in general and then applied to models of Hubbard Brook later.

[1] Manuscript received 14 December 1978; revised 15 August 1979; accepted 27 August 1979.

System definition and definition of terms

One may consider an ecological system to be composed of separate homogeneous entities or components. Patten et al. (1976) have used Koestler's (1967) term holon to refer to these entities. A system H is composed of n holons H_k, k = 1, . . . , n. Each holon may have associated with it several state variables. In this paper state variables will be assumed to represent storages of nutrients or energy and each holon, H_k, will have only one state variable, x_k, associated with it. Each holon H_k may receive inputs z_{k0} from the environment and donate outputs y_{0k} to the environment. Within the system H, flows of nutrients f_{ij} pass from H_j to H_i. Fig. 1 shows the relationship of these variables to each other. Derivatives $\dot{x}_k$ of each state variable x_k with respect to time ($\dot{x}_k = dx_k/dt$) are equal to inflows to H_k minus outflows from H_k:

$$\dot{x}_k = \sum_{j=1}^{n} f_{kj} + z_{k0} - y_{0k} - \sum_{i=1}^{n} f_{ik}. \qquad (1)$$

All variables are functions of time.

Throughflow

Throughflow T_k of holon H_k is defined as the sum of all flows into H_k minus the change in state (storage) if it is negative (or equivalently, the sum of all flows out of H_k plus the change in state if it is positive). This definition treats negative state derivatives as inflows and positive state derivatives as outflows. Thus, T_k represents the instantaneous rate at which matter or energy is moving through H_k. In equation form

$$T_k = \sum_{j=1}^{n} f_{kj} + z_{k0} - (\dot{x}_k)_- = \sum_{i=1}^{n} f_{ik} + y_{0k} + (\dot{x}_k)_+ \quad (2)$$

where f_{ij} is the flow from H_j to H_i,

$$(\dot{x}_k)_- = \begin{cases} 0 & \text{if } \dot{x}_k \geq 0 \text{ and} \\ \dot{x}_k & \text{if } \dot{x}_k < 0 \end{cases} \quad (3)$$

and

$$(\dot{x}_k)_+ = \begin{cases} \dot{x}_k & \text{if } \dot{x}_k > 0 \text{ and} \\ 0 & \text{if } \dot{x}_k \leq 0 \end{cases} \quad (4)$$

Total system throughflow, TST, is the sum of all throughflow in the system.

$$TST = \sum_{k=1}^{n} T_k. \quad (5)$$

TST can be considered the mobile pool in H at a particular time.

Total inflow to the mobile pool, including negative state derivatives, is defined as

$$\sum \text{IN} = \sum_{i=1}^{n} z_{i0} - \sum_{i=1}^{n} (\dot{x}_i)_-. \quad (6)$$

Total outflow from the mobile pool, including positive state derivatives is defined as

$$\sum \text{OUT} = \sum_{j=1}^{n} y_{0j} + \sum_{j=1}^{n} (\dot{x}_j)_+. \quad (7)$$

It should be noted that Σ IN and Σ OUT are always equal (Finn 1977), even when the system is not in steady state ($\dot{x}_j \neq 0$, for some j).

Inverse matrices

For a complete derivation of these equations see Finn (1977). If each flow f_{ij} is expressed as a fraction q^*_{ij} of the total flow entering H_i, then throughflow can be expressed as

$$T_j = \sum_{i=1}^{n} f_{ij} + y_{0j} + (\dot{x}_j)_+ = \sum_{i=1}^{n} q^*_{ij} T_i + y_{0j} + (\dot{x}_j)_+. \quad (8)$$

In matrix form

$$\boldsymbol{T}' = \boldsymbol{T}' Q^*_{22} + \boldsymbol{y}' + (\dot{\boldsymbol{x}})_+'$$

where $\boldsymbol{T}'$ is a row vector of throughflows, $\boldsymbol{y}'$ is a row vector of outflows, $(\dot{\boldsymbol{x}})'_+$ is a row vector of positive state derivatives, and Q^*_{22} is an $n \times n$ matrix of fractions q^*_{ij}. Q^*_{22} is the central portion of a larger matrix Q^* which contains the fractional contributions of inflows and negative state derivatives to holons, holons to outflows and positive state derivatives, as well as interholon contributions (Finn 1977). Solving for $\boldsymbol{T}'$ gives

$$\boldsymbol{T}' = [\boldsymbol{y}' + (\dot{\boldsymbol{x}})'_+] [I - Q^*_{22}]^{-1}. \quad (9)$$

Let the inverse matrix $[I - Q^*_{22}]^{-1}$ be called N^*_{22}. Eq. 9 relates the throughflow vector to components attributable to each outflow and each positive state derivative. The (i,j) element of N^*_{22} represents the amount of flow in H_j due to a unit of flow ending in (or leaving) H_i.

Alternatively, if each flow f_{ij} is expressed as a fraction q^{**}_{ij} of the total flow leaving H_j, then throughflow can be expressed as

$$T_j = \sum_{j=1}^{n} f_{ij} + z_{i0} - (\dot{x}_i)_- = \sum_{j=1}^{n} q^{**}_{ij} T_j + z_{i0} - (\dot{x}_i)_-. \quad (10)$$

In matrix form

$$\boldsymbol{T} = Q^{**}_{22} \boldsymbol{T} + \boldsymbol{z} - (\dot{\boldsymbol{x}})_- \quad (11)$$

where $\boldsymbol{T}$ is a column vector of throughflow, $\boldsymbol{z}$ is a column vector of inflows, $(\dot{\boldsymbol{x}})_-$ is a column vector of negative state derivatives and Q^{**}_{22} is an $n \times n$ matrix of fractions q^{**}_{ij}. Solving for $\boldsymbol{T}$ gives

$$\boldsymbol{T} = [I - Q^{**}_{22}]^{-1} [z - (\dot{x})_-] \quad (12)$$

Let the inverse matrix $[I - Q^{**}_{22}]^{-1}$ be called N^{**}_{22}. Eq. 12 relates the throughflow vector to components attributable to each inflow and negative state derivative. The (i,j) element of N^{**}_{22} represents the amount of flow in H_i due to a unit of flow starting in H_j (or entering H_j).

These inverse matrices allow one to construct flow diagrams for each inflow and outflow in the system. The i[th] row of N^*_{22} represents the throughflow vector due to one unit of y_{0i} [or positive state derivative $(\dot{x}_i)_+$].Interholon flows for a unit y_{0i} are calculated by multiplying the (i,k) element of N^*_{22} by the k[th] row of Q^*_{22}, for k = 1,n. The j[th] column of N^{**}_{22} represents the throughflow vector generated by one unit of inflow z_{j0} (or negative state derivative $(\dot{x}_j)_-$). Interholon flows for a unit z_{j0} are calculated by multiplying the (k,j) element of N^{**}_{22} by the k[th] column of Q^{**}_{22}, for k = 1,n.

Path length

Path length is defined as the average number of holons that an inflow or outflow passes through. For a unit of flow entering an ecosystem a portion may leave immediately, a portion may flow through several holons and then leave and a portion may cycle through the same holons many times before leaving. The average number of holons visited by all of these portions is the path length. The mean path length for the entire system $\overline{PL}$ is given by Finn (1976, 1977):

$$\overline{PL} = TST/\Sigma\ \text{IN} = TST/\Sigma\ \text{OUT}. \quad (13)$$

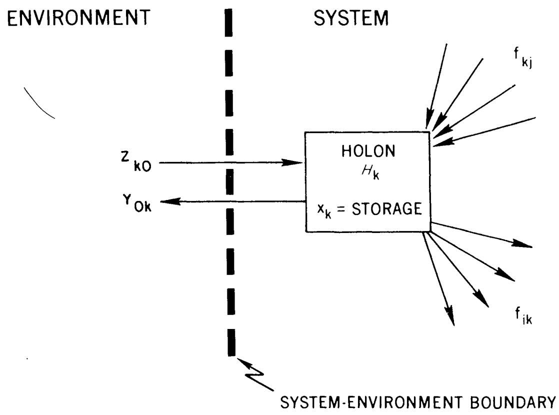

FIG. 1. Definition of terms. This diagram illustrates the meaning of the variables used in the text by showing all variables for one particular holon, H_k. The boundary between system and environment is crossed by z_{k0}, flowing into H_k, and by y_{0k}, flowing out of H_k. The variables f_{kj} represent flow of matter or energy from any of the holons H_j in the system (j = 1,n) to H_k. The variables f_{ik} represent flow from H_k to any holon H_i in the system (i = 1,n). Storage within holon H_k is represented by the variable x_k. The rate of change of x_k is denoted dx_k/dt or $\dot{x}_k$ and is the sum of all flows into H_k minus the sum of all flows out of H_k (Eq. 1).

In an ecosystem model, path length may be affected by the number of trophic levels, amount of cycling, system complexity and model resolution. Path length is the average length (in holons) of the paths taken through the system from inflow to outflow by a unit of energy or matter.

Cycling index

For each holon H_k, cycling efficiency RE_k may be defined as the fraction of throughflow T_k that returns to H_k (or the fraction that has already been in H_k). Rigler (1975) has a similar definition. In other words, cycling efficiency is the fraction of flow through a holon that returns, directly or indirectly, to that holon.

Cycling efficiency may be found by examining the diagonals of N^* and N^{**}. The diagonal element n^{**}_{kk} represents the amount of flow in H_k generated by a unit of flow starting in H_k. Thus, cycling efficiency is

$$RE_k = \frac{n^{**}_{kk} - 1}{n^{**}_{kk}} \quad (14)$$

since $(n^{**}_{kk} - 1)$ is the relative amount cycled (one unit started in H_k) and n^{**}_{kk} is the total relative throughflow.

The cycling index CI for the entire system is defined as the fraction of total system throughflow that is cycled. The cycled portion of total system throughflow is

$$TST_c = \sum_{k=1}^{n} RE_k T_k. \quad (15)$$

Cycling index is

$$CI = TST_c/TST. \quad (16)$$

Cycling index may vary from zero to one, zero meaning that there is no cycling at all (none of the flow through a holon returns directly or indirectly) and one meaning that all flow is cycled.

Straight-through path length

Because total system throughflow cycled, TST_c, is known (Eq. 15), it is possible to define the portion of total system throughflow that passes straight through the system as

$$TST_s = TST - TST_c. \quad (17)$$

From this and the definition of path length (Eq. 13) path length due to flow passing straight through the system, or straight-through path length $\overline{PL}_s$, can be defined as

$$\overline{PL}_s = TST_s/\Sigma \text{ IN} = TST_s/\Sigma \text{ OUT}. \quad (18)$$

Path length due to cycling can be defined similarly as

$$\overline{PL}_c = TST_c/\Sigma \text{ IN} = TST_c/\Sigma \text{ OUT}. \quad (19)$$

Straight-through path length is fairly stable for a given model structure. However, to compare straight-through path lengths for systems with different structures a relative measure should be used. One such measure is $\overline{PL}_s/\overline{PL}_s$ (MAX), where $\overline{PL}_s$ (MAX) is the maximum attainable straight-through path length for a given model structure. $\overline{PL}_s$ (MAX) is very difficult to determine for certain systems and so n is used as the maximum possible path length for any n holon model, even though most models cannot attain $\overline{PL}_s = n$. So a relative measure of straight-through path length in this paper will be $\overline{PL}_s/n$.

Summary of flow measures

Total system throughflow, TST, is the sum of all throughflows in a system. Unlike primary productivity or total inflow, TST counts each flow each time it passes through a component. It can be considered a measure of the activity of the system.

Cycling efficiency, RE_k, is the fraction of flow through a holon that will eventually (directly or indirectly) return to that holon. Cycling is thus defined with respect to each holon. Cycling index, CI, for a system is the fraction of total system throughflow that is cycled. It is essentially an average of the cycling efficiencies of each holon, weighted by the throughflow of each holon. Cycling index is a relative measure of cycling for the whole system. It allows comparison of cycling between models of different structure and between elements.

Path length $\overline{PL}$ is the average number of holons that an average inflow will pass through (or that an outflow has passed through). A portion of path length can be attributed to flows passing straight through the system,

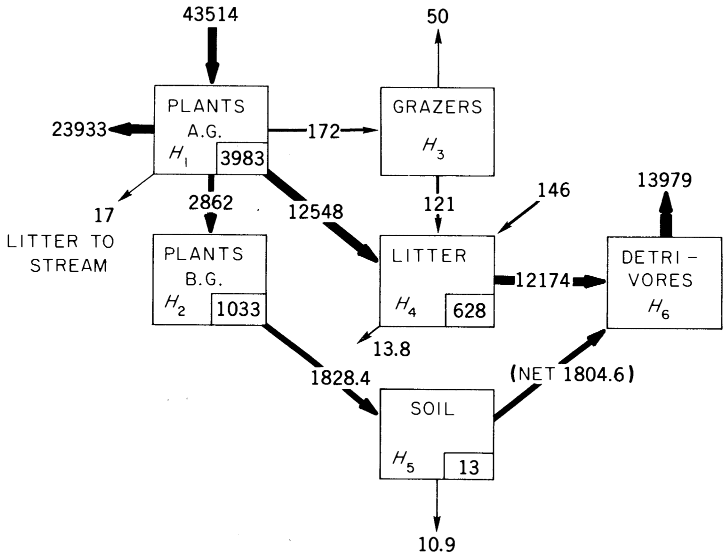

FIG. 2. Energy flow at Hubbard Brook, from Gosz et al. (1978). Flows are in kJ·m^{-2}·yr^{-1} (kilojoules per square metre per year). Holons are: H_1—aboveground plants, H_2—belowground plants, H_3—grazers, H_4—litter, H_5—soil, and H_6—detritivores. Numbers within boxes represent rate of energy accumulation in kJ·m^{-2}·yr^{-1}.

$\overline{PL}_S$. The remainder is attributable to cycled flows, $\overline{PL}_C$. Since the maximum straight-through path length for any model of n holons is n, a relative measure of path length useful for comparing different models is $\overline{PL}_S/n$.

ENERGY MODEL

A slightly modified version of the model of energy flow at Hubbard Brook presented by Gosz et al. (1978) is shown in Fig. 2. This arrangement has no loops, and, thus, must have a cycling index of zero. However, this is misleading as there is probably a loop between soil organic matter and detritivores, and between litter and detritivores. For the model as shown, $\overline{PL}$ = 1.72 and CI = 0.0.

As for most energy models studied (Finn 1977), path length is quite short. An average unit of energy does not even pass through two components of the system ($\overline{PL} < 2$). The large outflow from aboveground plants (totaling 23 949 kJ·m^{-2}·yr^{-1}) and the positive increment in storage 3983 kJ·m^{-2}·yr^{-1}) dominate the rest of the flows in the system. It appears to be generally true that energy flow systems which include autotrophs have path lengths < 2 (Finn 1977). This is because of the large respiration losses of autotrophs and heterotrophs at each trophic level, and the small amount of energy cycling. However, some heterotrophic systems (oyster beds, for example) have longer path lengths, because autotrophic respiration is not included, and detritus is cycled several times by various organisms.

TABLE 1. Flows for the Hubbard Brook model (Likens et al. 1977). All flows are in kg·ha^{-1}·yr^{-1}. z_{i0} is inflow to H_i from the environment, f_{ij} is flow from H_j to H_i, y_{0j} is outflow from H_j to the environment and $\dot{x}_i$ is the derivative of element storage in H_i. See Fig. 3.

	Ca	Mg	Na	K	S	N	P
z_{10}	0	0	0	0	6.1	0	0
z_{30}	0	0	0	0	0	14.2	0
z_{40}	2.2	0.6	1.6	0.9	12.7	6.5	0.04
f_{12}	52.8	8.3	0.43	52.7	21.5	68.3	5.6
f_{24}	62.2	9.3	34.8	64.3	24.5	79.6	8.9
f_{31}	40.7	5.9	0.1	18.3	5.8	54.2	4.0
f_{32}	3.2	0.5	0.01	2.1	0.6	6.2	1.7
f_{41}	6.7	2.0	0.3	30.1	21.0	9.3	0.7
f_{42}	3.5	0.2	34.2	8.0	1.9	0.9	0.2
f_{43}	42.4	6.1	0.1	20.1	5.7	66.9	5.2
f_{45}	21.1	3.5	5.8	7.1	0.8	6.5	2.77
y_{03}	0.1	0.1	0	0	0	0	0
y_{04}	13.7	3.1	7.2	1.9	17.6	3.9	0.01
y_{05}	0.2	0.2	0.2	0.5	0.1	0.1	0.01
$\dot{x}_1$	5.4	0.4	0.03	4.3	0.8	4.8	0.9
$\dot{x}_2$	2.7	0.3	0.12	1.5	0.4	4.2	1.4
$\dot{x}_3$	1.4	0.2	0.02	0.3	0.8	7.7	0.5
$\dot{x}_4$	0	0	0	0	0	0	0
$\dot{x}_5$	−21.3	−3.7	−6.0	−7.8	−0.9	−0.1	−2.78

NUTRIENT MODELS

Models from the Hubbard Brook ecosystem study

Fig. 3 shows the general model of nutrient cycling at Hubbard Brook presented by Likens et al. (1977), with flows for seven nutrients presented in Table 1. Path length and cycling index for these models are presented in Table 2. Both $\overline{PL}$ and CI are much higher for these models than for the energy model, again reflecting the effect of respiration and little or no cycling of energy. Straight-through path lengths, $\overline{PL}_S$, of the nutrient models are only about double that of the energy model, however.

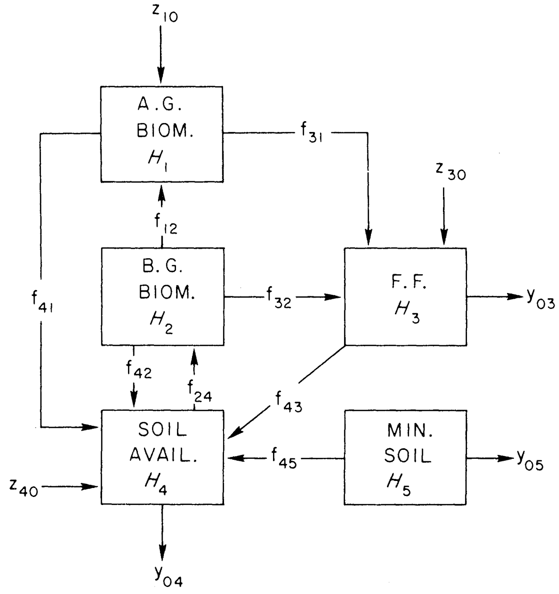

FIG. 3. General nutrient flow model of Hubbard Brook, adapted from Likens et al. (1977). Flows for seven different elements are presented in Table 1. Holons are H_1—aboveground biomass, H_2—belowground biomass, H_3—forest floor ($F + H$ layers), H_4—available nutrient pool, and H_5—mineral soil. z_{i0} is inflow to H_i from the environment, f_{ij} is flow from H_j to H_i, and y_{0j} is outflow from H_j to the environment.

The nutrients at Hubbard Brook appear to cycle in the following order: K > Na > N > Ca > P > Mg > S. This ordering relates to the input of each element from outside the system, the mobility of each element within the system, and the biological requirements of the organisms. The ordering observed here indicates that mobility, as represented by the lyotropic series, is a major factor in cycling. This will be discussed more fully later.

Path length does not rank the elements in the same order (K > N > P > Na > Ca > Mg > S) as cycling index (above) or straight-through path length (P > K > Ca > Mg > N > Na > S). The path length ranking is a composite of the cycling index ranking and the straight-through path length ranking. Rank for $\overline{PL}_s$ will be considered later.

TABLE 3. Inverse matrices for Ca model of Likens et al. (1977). Numbers are normalized to a unit outflow for the N^*_{22} matrix (row i corresponds to y_{0i}) and a unit inflow for the N^{**}_{22} matrix (column j corresponds to z_{j0}).

a. N^*_{22} matrix. Row 4 contains throughflow values for a unit outflow of Ca from H_4 (Fig. 4b).

	H_1	H_2	H_3	H_4	H_5
H_1	2.98	3.26	1.82	3.26	0.91
H_2	1.98	3.26	1.82	3.26	0.91
H_3	2.90	3.26	2.82	3.26	0.91
H_4	1.98	2.26	1.82	3.26	0.91
H_5	0	0	0	0	1.0

b. N^{**}_{22} matrix. Column 4 contains throughflow values for a unit inflow of Ca to H_4 (Fig. 4a).

	H_1	H_2	H_3	H_4	H_5
H_1	2.98	2.77	2.19	2.27	2.24
H_2	2.33	3.26	2.58	2.67	2.64
H_3	2.41	2.30	2.82	1.88	1.87
H_4	2.84	2.75	3.15	3.26	3.23
H_5	0	0	0	0	1.0

The pattern of flow through the system is revealed in the inverse matrices N^*_{22} and N^{**}_{22}. The elements N, P, K, Ca, and Mg cycle through all the loops in the system evenly. This results in N^*_{22} and N^{**}_{22} matrices with all but the fifth row nonzero and most entries about the same size (Table 3). Fig. 4a shows the flows resulting from one unit of Ca entering H_4 via precipitation, i.e., it traces where one unit of z_{40} goes. In these flow diagrams, the numbers inside the boxes represent throughflow. Arrows marked $\dot{x}_i$ represent state derivatives (increases or decreases in storage). Inflow z_{40} does not visit holon H_5 (mineral soil), but visits the remaining holons about twice each. About 60% of z_{40} leaves the system through outflow y_{04} (dissolved inorganic Ca export). A tiny fraction leaves as particulate matter, and the remainder is stored in H_1, H_2,

TABLE 2. Flow analysis measures for Hubbard Brook models. n is the number of holons in the model. TST is total system throughflow, Σ IN is the sum of inflows minus negative state derivatives (both TST and Σ IN are in the indicated units). $\overline{PL}$ is path length, $\overline{PL}_s$ is straight-through path length, $\overline{PL}_s/n$ is normalized straight-through path length and CI is cycling index (all of these measures are unitless).

			n	Σ IN	TST	$\overline{PL}$	$\overline{PL}_s$	$\overline{PL}_s/n$	CI
Energy	$kJ \cdot ha^{-1} \cdot yr^{-1}$	Gosz et al. 1978	6	43 660	75 170	1.7	1.7	0.29	0.000
Ca	$kg \cdot ha^{-1} \cdot yr^{-1}$	Likens et al. 1977	5	23.5	256.1	10.8	4.1	0.83	0.621
Mg	$kg \cdot ha^{-1} \cdot yr^{-1}$	Likens et al. 1977	5	4.3	40.1	9.3	3.8	0.76	0.592
Na	$kg \cdot ha^{-1} \cdot yr^{-1}$	Likens et al. 1977	5	7.6	83.3	11.0	2.6	0.53	0.759
K	$kg \cdot ha^{-1} \cdot yr^{-1}$	Likens et al. 1977	5	8.5	211.4	24.3	4.3	0.86	0.826
S	$kg \cdot ha^{-1} \cdot yr^{-1}$	Likens et al. 1977	5	19.7	101.5	5.2	2.5	0.51	0.507
N	$kg \cdot ha^{-1} \cdot yr^{-1}$	Likens et al. 1977	5	20.8	306.2	14.7	3.6	0.72	0.758
P	$kg \cdot ha^{-1} \cdot yr^{-1}$	Likens et al. 1977	5	2.8	31.9	11.3	4.5	0.89	0.605
Ca	$kg \cdot ha^{-1} \cdot yr^{-1}$	Jordan et al. 1972	4	12.0	200.3	16.7	3.4	0.85	0.797
Ca	$kg \cdot ha^{-1} \cdot yr^{-1}$	Waide et al. 1974	4	11.6	168.3	14.5	3.4	0.86	0.764

TABLE 4. N^{**}_{22} matrices. Numbers are normalized to a unit inflow (column j corresponds to z_{j0}).

a. N^{**}_{22} matrix for Na model. Column 4 contains throughflow values for a unit inflow of Na to H_4, z_{40} (Fig. 5a).

	H_1	H_2	H_3	H_4	H_5
H_1	1.05	0.07	0.05	0.06	0.06
H_2	4.21	5.70	3.94	4.72	4.57
H_3	0.24	0.02	1.01	0.02	0.01
H_4	5.08	5.67	4.75	5.70	5.51
H_5	0	0	0	0	1.0

b. N^{**}_{22} matrix for S model. Column 4 contains throughflow values for a unit inflow of S to H_4, z_{40} (Fig. 5b).

	H_1	H_2	H_3	H_4	H_5
H_1	2.06	1.93	0.98	1.12	1.0
H_2	1.20	2.19	1.12	1.27	1.13
H_3	0.46	0.46	1.23	0.27	0.24
H_4	2.07	2.04	1.92	2.19	1.94
H_5	0	0	0	0	1.0

and H_3. The pattern of flow for Ca outflow y_{04} is similar (Fig. 4b), except that H_5 (mineral soil) donates 91% of the outflow y_{04}. Fig. 4c traces where one unit of nitrogen inflow z_{30} (N fixation) goes. The throughflows are a little bigger than for Ca (there is more cycling) but the pattern of cycling is the same as that of Ca. The pattern of flow through the system for N inflow in precipitation (z_{40}) is almost identical to that for N fixation (Fig. 4c). This is because cycling is large compared to inflows and outflows so that the origin of the nitrogen scarcely makes a difference.

Sodium and sulfur exhibit different flow patterns. Table 4 shows N^{**}_{22} matrices for the Na and S models. Like the matrices in Table 3, the off-diagonal entries of the fifth row are zero. Unlike the other elements, rows 1 and 3 of the N^{**}_{22} matrix for Na are almost zero, and row 3 of the N^{**}_{22} matrix for S is small compared to rows 1, 2, and 4. Thus, unless introduced into them directly, sodium will hardly visit holons 1 or 3 (aboveground biomass or forest floor), and sulfur will probably not visit holon 3 (forest floor). Fig. 5a shows how one unit of Na inflow z_{40} (precipitation) flows through the system. There is a large exchange between belowground biomass (H_2) and available Na in soil (H_4), but the rest of the holons carry

→

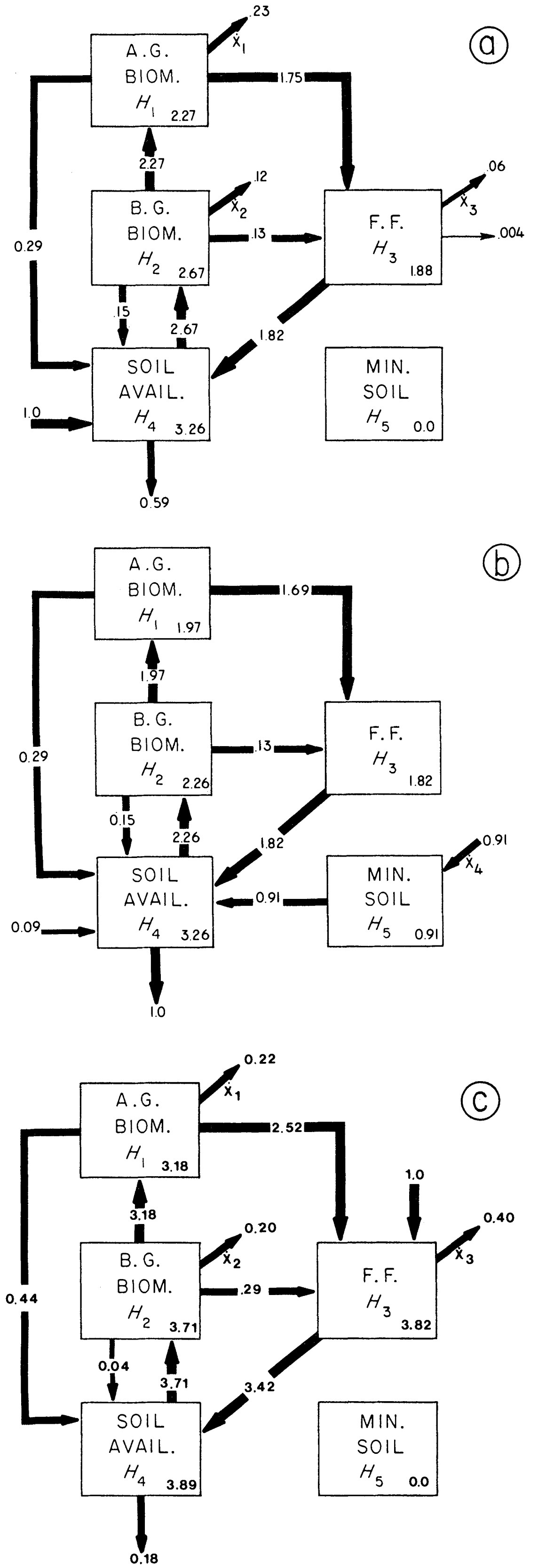

FIG. 4. Flow diagrams. All flows are relative to a unit of inflow (for a and c) or a unit of outflow (for b). Numbers within the boxes are throughflows due to the unit inflow (or outflow). See text for further explanation. (a) Ca inflow z_{40}. Throughflows are given in column 4 of the N^{**}_{22} matrix for Ca, Table 3b. (b) Ca outflow y_{04}. Throughflows are given in row 4 of the N^{*}_{22} matrix, Table 3a. (c) Nitrogen inflow z_{30}. Throughflows are from column 3 of the N^{**}_{22} matrix for the nitrogen model.

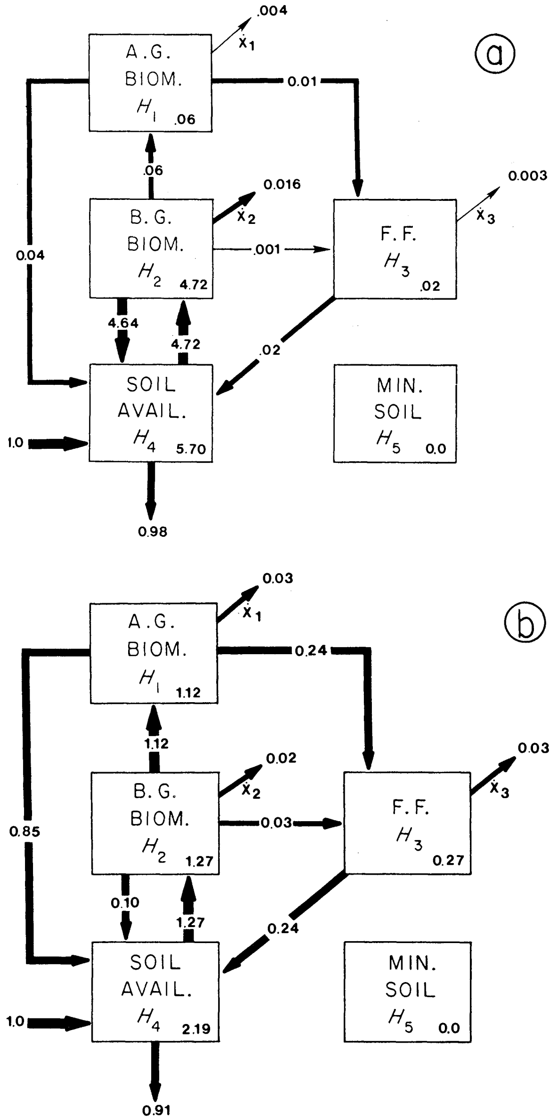

FIG. 5. Flow diagrams. All flows are relative to a unit inflow. Numbers within boxes are throughflows due to the unit inflow. See text for further explanation. (a) Na inflow z_{40}. Throughflows are from column 4 of the N^{**}_{22} matrix for Na, Table 4a. (b) S inflow z_{40}. Throughflows are from column 4 of the N^{**}_{22} matrix for S, Table 4b.

almost no sodium. Fig. 5b shows how one unit of S inflow z_{40} flows through the system. Most of the cycling for sulfur is from available soil S (H_4) through both biomass components and back to H_4 through stemflow and throughfall, bypassing the forest floor H_3 (in this model structure).

Other Ca models

Fig. 6 shows a model of Ca cycling at Hubbard Brook presented by Jordan et al. (1972). Unlike the model of Likens et al. (1977) this model is in steady state. $\overline{PL}$ and CI (Table 2) are both higher for this

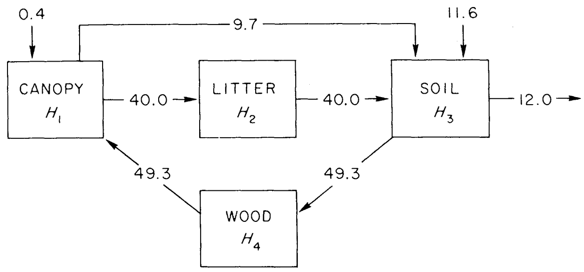

FIG. 6. Calcium flow at Hubbard Brook, from Jordan et al. (1972). Flows are in kg Ca·ha^{-1}·yr^{-1}. Holons are H_1—canopy, H_2—litter, H_3—soil, and H_4—wood including roots.

version of the Ca cycle at Hubbard Brook than for the version of Likens et al. (1977). This is at least in part due to the steady state assumption. Flow analysis treats state derivatives as inflows or outflows and this adds at least 9.5 kg Ca·ha^{-1}·yr^{-1} to the outflow of Likens' model.

Fig. 7 shows a model of Ca cycling at Hubbard Brook presented by Waide et al. (1974). Path length and cycling index (Table 2) are higher for this version of the Hubbard Brook Ca cycle than for Likens' version. This model is also in steady state.

Comparison of Ca models

The difference in path length and cycling for the three different Hubbard Brook Ca models is due to differences in model formulation and structure, and differences in Ca flows through the system. The data used by Jordan et al. (1972) and Waide et al. (1974) was not as complete as that used by Likens et al. (1977). If flows presented by Likens et al. (1977) are used for all three model structures, then differences in path length and cycling can be attributed to model structure alone.

The models have the following structural differences. First Waide et al. had one vegetation holon; Likens et al. divided vegetation into above- and belowground; and Jordan et al. divided vegetation into wood and canopy. Waide and Likens included rock and soil minerals; Jordan did not. The remaining differences are removed by using Likens' flow data. Waide and Jordan included weathering as an input; Likens did not. Waide had all rain and throughfall pass through litter; Jordan and Likens did not. Likens included the contribution of roots to litter, and flow of root exudates to the available nutrient pool; Jordan and Waide did not.

Table 5 shows values of Ca flow for the models of Jordan et al. (1972) and Waide et al. (1974) that are equivalent to the flows presented by Likens et al. (1977) (Table 1, column 1). Flow measures for the modified and original models are presented in Table 6.

Differences among the three different model structures have been considerably reduced. Path lengths

TABLE 5. Flows for Ca models equivalent to the flows presented by Likens et al. (1977). See Fig. 5 for Jordan et al. (1972) and Fig. 6 for Waide et al. (1974).

Jordan et al. (1972)	Waide et al. (1974)
$z_{30} = 23.3$	$z_{30} = 2.2$
$y_{02} = 0.1$	$y_{02} = 0.1$
$y_{03} = 13.9$	$y_{03} = 13.7$
$f_{14} = 47.4$	$y_{04} = 0.2$
$f_{31} = 6.7$	$f_{13} = 62.2$
$f_{21} = 40.7$	$f_{21} = 43.9$
$f_{34} = 3.5$	$f_{31} = 10.2$
$f_{43} = 62.2$	$f_{32} = 42.4$
$f_{32} = 42.4$	$f_{34} = 21.1$
$f_{24} = 3.2$	$\dot{x}_1 = 8.1$
$\dot{x}_1 = 0.0$	$\dot{x}_2 = 1.4$
$\dot{x}_2 = 1.4$	$\dot{x}_3 = 0.0$
$\dot{x}_3 = -0.2$	$\dot{x}_4 = -21.3$
$\dot{x}_4 = 8.1$	

are now within a range of two instead of six. This change was not due to straight-through path length which changed very little. Cycling indices now fall within a range of .07 instead of .18. Remaining differences are due to the structural differences of the models. It is remarkable how similar these indices are considering the basic differences in model architecture.

DISCUSSION

Flow analysis of several models of the Hubbard Brook Ecosystem has produced results which sometimes confirmed the obvious but often proved interesting.

It was expected that the metabolic energy flow model should show low values of path length and cycling, compared to the mineral cycling models because energy tends to flow straight through a system and because of large respiration losses at each trophic level (Odum 1971). Even if a large portion of organic matter cycles from detritus to detritivores (coprophagy and multiple processing of detritus), this would not increase $\overline{PL}$ and CI for energy much because of the overwhelming effect of plant and animal respiration. Despite recent argument (Rigler 1975), energy flows one way with very little cycling.

There is a large variation in behavior of nutrient elements in the biogeochemistry of Hubbard Brook. Patterns are not immediately obvious in the various flow measures. Of the seven elements studied, N and P are limiting elements, K, Ca, Mg, and S are nonlimiting essential elements, and sodium is nonessential (for plants). The only flow measures that differentiate Na from the other elements are straight-through path length and normalized straight-through path length (Table 2). Sodium and sulfur differ markedly from the other elements in their pattern of flow through the system. Sodium cycles from the available nutrient pool (H_4) to belowground biomass (H_2) and back, almost exclusively (Fig. 5a). Sulfur travels from available nutrients (H_4) up through vegetation (H_2 and H_1) and is leached out of the canopy (Fig. 5b); only ≈21% of the sulfur taken up by aboveground biomass falls to the forest floor in litter. By contrast, Ca visits all four nonmineral holons (Fig. 4a), as do the rest of the elements. These differences in flow pattern are reflected in straight-through path length. Likens et al. (1977, page 102) observed the different paths taken by sodium and sulfur compared to the other elements.

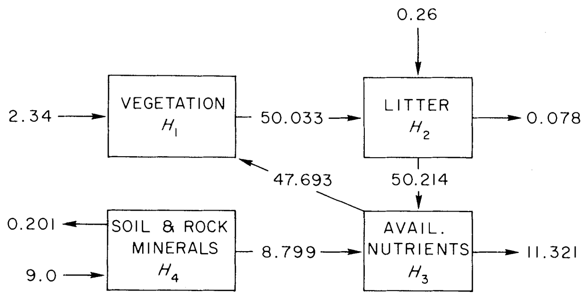

FIG. 7. Calcium flow at Hubbard Brook, from Waide et al. (1974). Flows are in kg Ca·ha^{-1}·yr^{-1}. Holons are H_1—vegetation, H_2—litter, H_3—available nutrients, and H_4—soil and rock minerals.

The rank order of the elements in cycling index (K > Na > N > Ca > P > Mg > S) is interesting in several ways. This order does not appear to relate to whether or not the system is gaining or losing a particular nutrient. Hubbard Brook is accumulating N, S, and P and losing Ca, Na, Mg, and K (Likens et al. 1977). However, if model boundaries are drawn differently to exclude rock and soil minerals, as in the Hubbard Brook model of Jordan et al. (1972) (Fig. 6), then all of these elements are being accumulated. The cations (K > Na > Ca > Mg) fall out in strict order of atomic size and charge, which are indices of mobility (the lyotropic series). It is surprising that Na is so high. One might have suspected that since Na is not necessary in large quantities for plant growth that plants would take up other cations instead. However, Na cycles almost as much as K and much more than Ca or Mg. This is not true in other forest systems where Na can have very low values for cycling index (Finn 1977). The relative position of K and Ca is understandable in terms of the biological role of these elements. Potassium is mobile, a part of fluids in the tissues, whereas Ca is structural, a constituent of cell walls and membranes. Unfortunately, the high Na value may be the result of contamination in root exudates (Smith 1976).

The order of the remaining elements (N > P > S) makes sense in terms of the relative requirements for them. Nitrogen is generally thought to be more limiting in temperate deciduous forests than phosphorus (Duvigneaud and Denaeyer-DeSmet 1975) while sulfur is not considered limiting at all, especially in the polluted Northeast.

Comparison of different models of Ca cycling for

TABLE 6. Flow measures for Ca models (see Table 2 for abbreviations).

	n	Σ IN	TST	$\overline{PL}$	$\overline{PL}_s$	$\overline{PL}_s/n$	CI
		kg Ca$\cdot$ ha$^{-1}\cdot$yr^{-1}	kg Ca$\cdot$ ha$^{-1}\cdot$yr^{-1}				
Likens et al. 1977	5	23.5	256.1	10.9	4.13	0.83	0.621
Jordan et al. 1972	5	12.0	200.3	16.7	3.39	0.85	0.797
Waide et al. 1974	4	11.6	168.3	14.5	3.43	0.86	0.764
Modified (flows in Table 6 equivalent to Likens et al. 1977)							
Jordan et al. 1972	4	23.5	229.6	9.8	3.17	0.79	0.676
Waide et al. 1974	4	23.5	203.3	8.7	3.37	0.84	0.610

Hubbard Brook is essentially a test of how robust the flow analysis measures are to changes in model structure and to changes in flows. The results in Table 6 indicate that flow measures are relatively insensitive to different assumptions about model structure, and more sensitive to change in flows and assumptions about steady state. Straight-through path length is the most robust of the flow measures, i.e., it is least sensitive to changes in model structure or flows.

The general question of the sensitivity of flow measures to structural changes in a model is far from resolved. Some classes of structural change have been examined in detail (Finn 1977). For example, a single holon can be split into an arbitrary number of parallel holons without changing any of the flow measures. This is true as long as no additional flows between the new holons are added. Thus, separating out similar species in a nutrient flow model should have no effect on flow measures. The sensitivity to small changes in boundary definition, choice of holons, and flow paths of flow measures and other measures of biogeochemical cycling, including input/output ratios, has not been addressed in detail.

How do flow measures presented in this paper relate to other measures of nutrient behavior? Four measures of nutrient behavior at Hubbard Brook presented by Whittaker et al. (1979) are listed in Table 7: (1) nutrient concentration in deciduous tree parts divided by nutrient concentration in woody parts, a measure of the enrichment of active tissues over inactive; (2) leachability (nutrients leached divided by nutrient stock in leaves); (3) relative turnover of aboveground stock (nutrients in litterfall plus leaching divided by aboveground stock in percent); and (4) relative turnover of NPP (nutrients in litterfall plus leaching divided by net primary production, in percent).

As determined by Spearman's rank correlation, none of the measures in Table 7 are signficantly related to CI, $\overline{PL}$, or $\overline{PL}_s/n$. Cycling index and $\overline{PL}$ are significantly correlated (Spearman's rank correlation = 0.82, $P < .05$), as are leachability and relative turnover of NPP (0.96, $P < .001$).

It is clear that leachability, turnover rate, and the "enrichment" of deciduous vs. woody parts all have some relationship to nutrient cycling in forest ecosystems. However, their relationship to nutrient cycling as measured by CI and the other flow measures is unclear. For example, turnover rate is a measure of the residence time of a nutrient atom in a component or system. Flow measures do not take into account residence times or storages, but only the amounts of nutrients actually moving and the way in which they move. This comparison of indices demonstrates that all the different processes involved in nutrient cycling cannot be captured and quantified in a single index. The flow measures presented in this paper do not merely mimic other nutrient behavior measures, but add new information for analysis.

Flow analysis offers a new set of tools to investigators of biogeochemical cycling which enables comparisons between elements and across systems, and which also may serve as an aid in evaluating models of cycling.

TABLE 7. Nutrient characterizations: ratios expressing nutrient behavior at Hubbard Brook, New Hampshire. Taken from Table 7 in Whittaker et al. (1979).

	Ca	Mg	Na	K	S	N	P
Deciduous/woody concentrations	2.2	6.4	1.5	10.2	6.0	10.0	8.0
Leachability (leaching/leaf pool)	.32	.38	5.75	.94	3.75	.13	.12
Relative turnover rate (litter + leaching)/aboveground stock, %	11.3	19.6	25.7	30.3	60.8	16.2	12.1
Relative turnover rate (litter + leaching)/aboveground NPP, 1961–1965, %	1.17	1.06	3.52	1.19	3.42	.637	.548

ACKNOWLEDGMENTS

Much of this work was performed while I was a graduate student at the University of Georgia, supported by a non-teaching assistantship from the Graduate School. My major professor, Dr. Bernard C. Patten, and many of my fellow graduate students including Gregor Auble, Craig Barber, Robert Bosserman, William Cale, David Hamilton, James Hill, and Jack Waide were very helpful in the development of flow analysis. I was supported during a portion of this work as a postdoctoral assistant with Dr. Daniel B. Botkin at the Ecosystem Center, Marine Biological Laboratory, Woods Hole, Massachusetts under a subcontract of the National Science Foundation grant for the Hubbard Brook Ecosystem Study, "Hydrologic Nutrient Cycle Interaction in Small Undisturbed and Man-Manipulated Ecosystems (Watersheds)." This publication is a contribution from the Hubbard Brook Ecosystem Study.

LITERATURE CITED

Barber, M. C. 1978*a*. A retrospective Markovian model of ecosystem resource flow. Ecological Modelling **5**:125–135.

———. 1978*b*. A Markovian model for ecosystem flow analysis. Ecological Modelling **5**:193–206.

Cale, W. G. 1975. Simulation and systems analysis of a shortgrass prairie ecosystem. Dissertation. University of Georgia, Athens, Georgia, USA.

Duvigneaud, P., and S. Denaeyer-DeSmet. 1975. Mineral cycling in terrestrial ecosystems. Pages 133–154 *in* Productivity of world ecosystems. National Academy of Sciences, Washington, District of Columbia, USA.

Finn, J. T. 1976. Measures of ecosystem structure and function derived from analysis of flows. Journal of Theoretical Biology **56**:363–380.

———. 1977. Flow analysis: a method for tracing flows through ecosystem models. Dissertation. University of Georgia, Athens, Georgia, USA.

———. 1978. Cycling index: a general definition for cycling in compartment models. Pages 138–164 *in* D. C. Adriano and I. L. Brisbin, editors. Environmental chemistry and cycling processes. DOE Symposium Series 45, CONF 760429. National Technical Information Service, Springfield, Virginia, USA.

Gosz, J. R., R. T. Holmes, G. E. Likens, and F. H. Bormann. 1978. The flow of energy in a forest ecosystem. Scientific American **238**(3):92–102.

Hannon, B. 1973. The structure of ecosystems. Journal of Theoretical Biology **41**:535–546.

Jordan, C. F., J. R. Kline, and D. S. Sasscer. 1972. Relative stability of mineral cycles in forest ecosystems. American Naturalist **106**:237–253.

Koestler, A. 1967. The ghost in the machine. MacMillan, New York, New York, USA.

Likens, G. E., F. H. Bormann, R. S. Pierce, J. S. Eaton, and N. M. Johnson. 1977. Biogeochemistry of a forested ecosystem. Springer-Verlag, New York, New York, USA.

Odum, E. P. 1971. Fundamentals of ecology. Third edition. W. B. Saunders, Philadelphia, Pennsylvania, USA.

Patten, B. C., R. W. Bosserman, J. T. Finn, and W. G. Cale. 1976. Propagation of cause in ecosystems. Pages 457–579 *in* B. C. Patten, editor. Systems analysis and simulation in ecology. Volume 4. Academic Press, New York, New York, USA.

Patten, B. C., and J. T. Finn. 1979. Systems approach to continental shelf ecosystems. Pages 183–212 *in* E. Halfon, editor. Theoretical systems ecology. Academic Press, New York, New York, USA.

Rigler, F. H. 1975. The concept of energy flow and nutrient flow between trophic levels. Pages 15–26 *in* W. H. van-Dobbin and R. H. Lowe-McConnel, editors. Unifying concepts in ecology. Junk, The Hague, Netherlands.

Smith, W. H. 1976. Character and significance of forest tree root exudates. Ecology **57**:324–331.

Waide, J. B., J. E. Krebs, S. P. Clarkson, and E. M. Setzler. 1974. A linear system analysis of the calcium cycle in a forested watershed ecosystem. Progress in Theoretical Biology **3**:261–345.

Whittaker, R. H., G. E. Likens, F. H. Bormann, J. S. Eaton, and T. G. Siccama. 1979. The Hubbard Brook Ecosystem Study: forest nutrient cycling and element behavior. Ecology **60**:203–220.

LINKED CITATIONS

Literature Cited

Relative Stability of Mineral Cycles in Forest Ecosystems
Carl F. Jordan; Jerry R. Kline; Donald S. Sasscer
The American Naturalist, Vol. 106, No. 948. (Mar. - Apr., 1972), pp. 237-253.
Stable URL:
http://links.jstor.org/sici?sici=0003-0147%28197203%2F04%29106%3A948%3C237%3ARSOMCI%3E2.0.CO%3B2-Z

Character and Significance of Forest Tree Root Exudates
William H. Smith
Ecology, Vol. 57, No. 2. (Mar., 1976), pp. 324-331.
Stable URL:
http://links.jstor.org/sici?sici=0012-9658%28197603%2957%3A2%3C324%3ACASOFT%3E2.0.CO%3B2-U

The Hubbard Brook Ecosystem Study: Forest Nutrient Cycling and Element Behavior
R. H. Whittaker; G. E. Likens; F. H. Bormann; J. S. Easton; T. G. Siccama
Ecology, Vol. 60, No. 1. (Feb., 1979), pp. 203-220.
Stable URL:
http://links.jstor.org/sici?sici=0012-9658%28197902%2960%3A1%3C203%3ATHBESF%3E2.0.CO%3B2-1